Regionalization of the Atmospheric Dust Cycle on the Periphery of the East Antarctic Ice Sheet Since the Last Glacial Maximum

G. Baccolo, B. Delmonte, Samuel Albani, C. Baroni, G. Cibin, M. Frezzotti, D. Hampai, A. Marcelli, Marie Revel, C. Salvatore, et al.

AGU100 ADVANCING EARTH AND SPACE SCIENCE

Geochemistry, Geophysics, Geosystems

RESEARCH ARTICLE
10.1029/2018GC007658

Key Points:
- The dust cycle reacted differently to the last climatic transition in different regions of the East Antarctic Ice Sheet
- The reduced transport of remote dust enhanced the emergence of a signal related to local dust dynamics in the Talos Dome ice core
- The chemical index of alteration provides constraints to track ice core dust provenance, also in relation to its formation environment

Supporting Information:
- Supporting Information S1

Correspondence to:
G. Baccolo,
giovanni.baccolo@mib.infn.it

Citation:
Baccolo, G., Delmonte, B., Albani, S., Baroni, C., Cibin, G., Frezzotti, M., et al. (2018). Regionalization of the atmospheric dust cycle on the periphery of the East Antarctic ice sheet since the Last Glacial Maximum. *Geochemistry, Geophysics, Geosystems*, *19*, 3540–3554. https://doi.org/10.1029/2018GC007658

Received 2 MAY 2018
Accepted 30 JUL 2018
Accepted article online 11 SEP 2018
Published online 28 SEP 2018

Regionalization of the Atmospheric Dust Cycle on the Periphery of the East Antarctic Ice Sheet Since the Last Glacial Maximum

G. Baccolo[1,2,3], B. Delmonte[2], S. Albani[4], C. Baroni[5,6], G. Cibin[7], M. Frezzotti[8], D. Hampai[9], A. Marcelli[9,10], M. Revel[11], M. C. Salvatore[5,6], B. Stenni[12], and V. Maggi[2,3]

[1]Graduate School in Polar Science, University of Siena, Siena, Italy, [2]Environmental and Earth Sciences Department, University Milano-Bicocca, Milan, Italy, [3]Milano-Bicocca section, INFN, Rome, Italy, [4]Laboratoire des Sciences du Climat et de l'Environnement, CEA-CNRS-UVSQ, Gif-sur-Yvette, France, [5]Earth Sciences Department, University of Pisa, Pisa, Italy, [6]CNR, Institute of Geosciences and Earth Resources, Pisa, Italy, [7]Diamond Light Source, Didcot, UK, [8]ENEA-, Rome, Italy, [9]INFN Laboratori Nazionali di Frascati, Frascati, Italy, [10]Rome International Center for Materials Science Superstripes, Rome, Italy, [11]Département Terre Environnement Espace, University of Nice Sophia Antipolis, Nice, France, [12]Department of Environmental Sciences Informatics and Statistics, Università Ca' Foscari-Venezia, Venice, Italy

Abstract Ice cores from inner East Antarctica provided some of the longest and most detailed climatic reconstructions and allowed understanding the relationships between atmospheric mineral dust and climate. In this work we present synchrotron radiation X-ray Fluorescence geochemical data of dust from the TALDICE ice core drilled at Talos Dome, a peripheral ice dome of East Antarctica (Western Ross Sea). Results highlight a dominant southern South American origin for dust at TALDICE during the Last Glacial Maximum, similarly to other sites located further inland onto the polar plateau. On the contrary, a different scenario concerns Talos Dome during the Holocene if it is compared to more inner sites. The tight connection between high southern latitudes and Antarctica that characterizes cold climate stages becomes weaker since the onset of the last climatic transition and throughout the Holocene. The net effect of this process at Talos Dome is a modification of the atmospheric and environmental settings, owing to local Antarctic sources of Victoria Land to gain importance and become the dominant ones. At the same time in inner East Antarctica the provenance of dust remains remote also during Holocene, revealing an evolution of the homogeneous scenario observed in glacial periods. The enhanced sensitivity of peripheral ice sheet sites to local dust sources makes Talos Dome an ideal site to assess the climatic and atmospheric changes of the peripheral sectors of East Antarctica during the current interglacial period.

Plain Language Summary During the Last Glacial Maximum, about 20,000 years ago, mineral dust from South America was massively transported toward Antarctica as a consequence of impressive environmental and climatic changes. Many ice cores drilled from the inner sectors of the Antarctic ice sheets support this scenario. Little is known when attention is shifted to peripheral areas and to interglacial periods. A new record of mineral particles at Talos Dome, a peripheral area of the East Antarctic ice sheet (Western Ross Sea sector), is here presented to partially close these gaps. Combining the data about concentration, composition, and grain size of the dust deposited at Talos Dome, it was possible to appreciate the influence played by local Antarctic dust sources to the depositional budget of the site. These local sources, corresponding to localized ice-free areas, are extremely important when attention is given to the peripheries of the ice sheets. This is particularly true for interglacial periods, when the transport and the deposition of mineral dust from South America to Antarctica is much reduced.

1. Introduction

Atmospheric mineral dust is an important component of Earth climate system. The comprehension of the dynamics governing the dust cycle on large temporal and spatial scales owes much to paleoclimatic archives (Martìnez-Garcia et al., 2011; Rea, 1994) and to polar ice cores. The latter allowed obtaining the most accurate records of the dust cycle during the Holocene and the Pleistocene (Kawamura et al., 2017; Lambert et al., 2008). The links between dust and climate are complex, but the general picture, thanks to these records, is

relatively well known (Albani et al., 2015; Maher et al., 2010; Marx et al., 2018). A key point revealed by ice cores is the correlation between dust concentration in ice and climatic conditions. The colder the climate, the higher is the amount of dust entrapped in ice, as a consequence of an increased atmospheric burden during cold climatic stages (Ridgwell & Watson, 2002). This evidence concerns long-term climatic variability as well as glacial-interglacial cycles (Lambert et al., 2008) and faster oscillations (Bory et al., 2010; Wegner et al., 2015). The connection results from many mechanisms interacting with each other: variations of the hydrological cycle and dust atmospheric lifetime, sea level changes, and environmental conditions at the dust sources, such as glacial activity or dryness (Petit & Delmonte, 2009; Yung et al., 1996). These factors explain why the deposition of dust in Antarctica during glacials is about 20 times higher than that during interglacials (Lambert et al., 2008; Yung et al., 1996). Dust also influences climate and many processes linked to climate: atmospheric chemistry and physics, radiative transfers, and biogeochemical cycles (Jickells et al., 2005; Maher et al., 2010; Marcelli & Maggi, 2017).

The inner East Antarctic Ice Sheet (EAIS) provided detailed dust records of the last 800,000 years (Lambert et al., 2008). Ice cores from this region showed that dust concentration is not the only parameter influenced by climate. Changes of the atmospheric circulation and environmental conditions over the continents modified also dust composition and grain size (Delmonte, Petit, et al., 2004; Delmonte et al., 2017; Gabrielli et al., 2005, 2010). Multiple lines of evidence point to a remote South American source for the dust deposited on EAIS during cold stages. It is supported by ice cores from inner and peripheral EAIS (Aarons et al., 2017; Delmonte, Andersson, et al., 2010; Delmonte, Basile-Doelsch, et al., 2004; Marino et al., 2009), by marine sediments (Weber et al., 2012), and by modeling constraints (Albani, Mahowald, et al., 2012; F. Li et al., 2008). In this respect, the role of the Argentinian emerged continental shelf as dust supplier in the Last Glacial Maximum (LGM), was recently raised (Delmonte et al., 2017). On the contrary, during interglacials dust provenance is less clear, mostly because of the low concentration of dust in Antarctic interglacial ice (no more than 10–20 ng_{dust}/g_{ice}). Despite these difficulties, clay mineralogy (Gaudichet et al., 1992), Sr-Nd isotopes (Revel-Rolland et al., 2006), and atmospheric models (Albani, Mahowald, et al., 2012) suggest that Australia could be an important source for dust deposited in inner EAIS during interglacials. However, a few data are available from peripheral EAIS, where the dust source during interglacial periods is still debated (Bory et al., 2010; Delmonte et al., 2013). The picture is even poorer considering the west Antarctic ice sheet, where preliminary observations, mainly from models, point to a composite origin during the Holocene (Koffman et al., 2014; Mahowald et al., 2010, 2011; McConnell et al., 2007; Neff & Bertler, 2015). These observations define a homogeneous picture for glacial periods, when climate and dust are coupled on a hemispheric scale (Lambert et al., 2008). During interglacials the connection is weaker, allowing regional dynamics to gain importance and become detectable (Aarons et al., 2016; Albani, Delmonte, et al., 2012; Bory et al., 2010). A record clearly showing such a transition is not yet available.

In this study we present a new updated data set concerning concentration, grain size, and composition of dust retrieved from the TALDICE ice core (TALos Dome ICE core) during the last 25 kyr, that is, the LGM (25–18 kyr BP, 1 kyr BP = 1,000 years Before Present, intended conventionally as 1950), the deglaciation (18–11.7 kyr BP), and the Holocene (11.7–0.7 kyr BP). Talos Dome (TD) is a peripheral ice dome at the edge of EAIS, near Victoria Land, in the western region of the Ross Sea area. Here several key components of the Antarctic system are found in close correspondence determining complex dynamics (Bertler et al., 2018; Mezgec et al., 2017). Focusing on the atmospheric dust, the Transantarctic Mountains, where limited but numerous ice-free sites occur (Delmonte, Baroni, et al., 2010), play an important role. They were mentioned to explain the anomalies in grain size, composition, and concentration of mineral particles deposited at TD (Albani, Delmonte, et al., 2012; Delmonte, Baroni¸ et al., 2010; Delmonte et al., 2013). Other low-altitude ice-free areas seem less important with respect to the TD sector of EAIS. Another feature influencing the dust cycle in the Ross Sea area is volcanism. Explosive eruptions from Antarctic volcanoes (see Figure 1) occurred throughout the Quaternary, locally spreading large amount of ash and tephra (Narcisi et al., 2012, 2016). The deposition of volcanic material across Victoria Land is particularly relevant in the Holocene, when background dust input at TD is characterized by a continuous volcanic contribution that prevents the interpretation of Sr-Nd isotope data (Delmonte et al., 2013). Given the complexity of the neighboring Ross Sea and Victoria Land regions, Talos Dome represents an ideal site to assess the impact of the last glacial-interglacial transition on the dust cycle in peripheral Antarctic areas, in opposition to the records from inner EAIS sites.

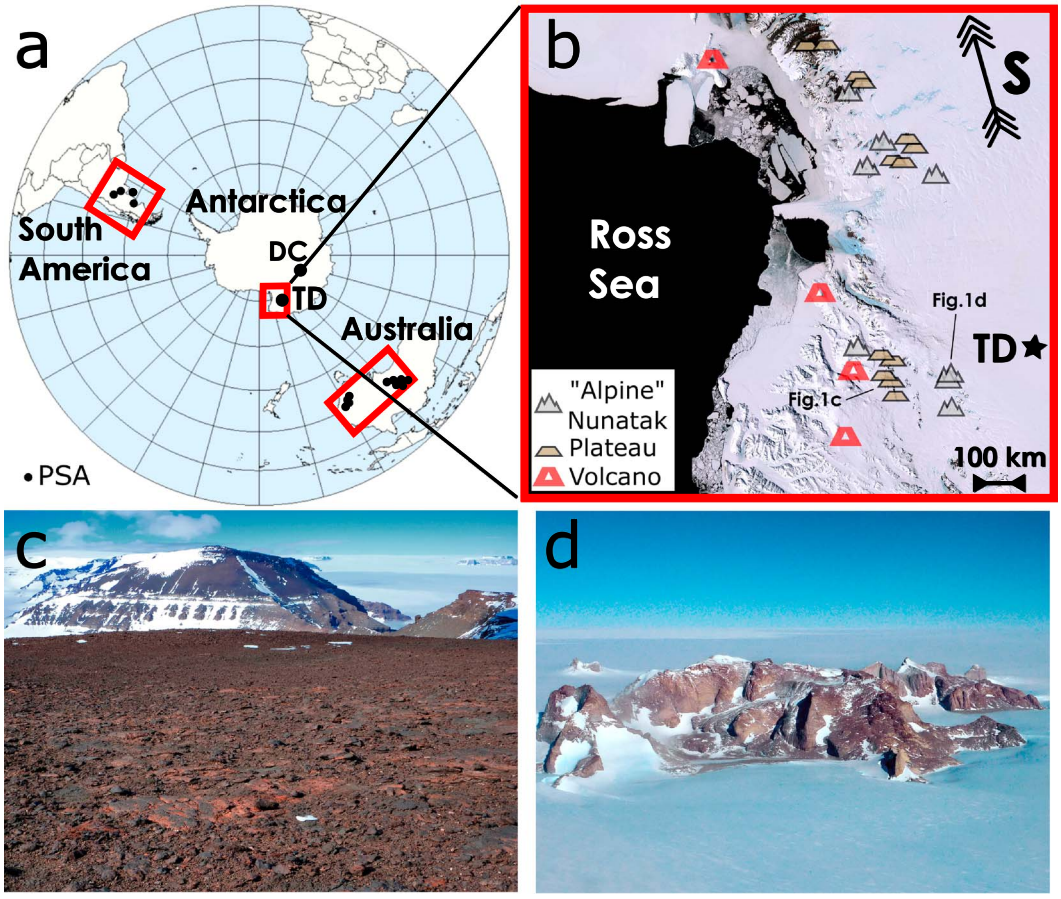

Figure 1. (a) The geographical setting of this work, including the location of the potential source areas. TD and DC refer to Talos Dome and Dome C. in part (b) a zoom of Victoria land with the Antarctic PSA considered here (divided in relation to their morphology) and the principal volcanoes of the region (from N to S: The Pleiades, Mount Rittmann, Mount Melbourne, and Mount Erebus). In parts (c) and (d) are two portrayals of typical potential source area ice-free sites of Victoria land. Part (c) shows a summit plateau (about 2,600 m) characterizing the doleritic Mesa range massif. Such plateaus are flat structural surfaces where the effect of weathering is easily appreciated. Part (d) refers to Frontier Mountain (aerial view from east), a granitic nunatak presenting a well-articulated alpine morphology, with defined peaks (maximum height 2,805 m) and glacial cirques.

2. Materials and Methods

2.1. TALDICE Ice Core and Ice Samples

The TD ice core is 1,620-m long; it was retrieved from the homonymous ice dome, at the northeastern edge of EAIS (2,315 m a.s.l., 159°11′E to 72°49′S, Figure 1). The proximity to the ocean is responsible for a high snow accumulation rate—present value 80 mm water equivalent per year (Frezzotti et al., 2004)—which allowed for obtaining a high temporal resolution record. The first 1,450 m of the core covers the Holocene, the last glacial period (MIS 2–4, Marine Isotopic Stage) and the previous interglacial one (MIS 5 and substages), corresponding approximately to the last 150 kyr (Stenni et al., 2011). The chronology adopted in this work is AICC2012; the average age uncertainty is between 150 and 300 years during Holocene, increasing to 500–1000 years during MIS 2 (Veres et al., 2013).

Ice samples from the Holocene, the deglaciation, and the LGM were considered. The preparation was carried out using clean devices in a class ISO 6 clean room, equipped with an ISO 5 laminar flow bench. The outer part of each strip was removed with three baths in ultrapure MilliQ water. After melting, meltwater was divided into two aliquots: one (8–10 ml) for particle concentration and size analyses and one for compositional analyses. In the second case dust was concentrated and extracted through filtration, using precleaned (nitric acid 5%, ultrapure grade) polycarbonate membranes (0.4 μm pore size). Meltwater from several ice samples was

merged and filtered, in order to make available at least 2–3 μg of dust on each membrane. A pipette was used to deposit meltwater on the membranes, so as to concentrate the filtered dust on the smallest possible area. Membranes were successively mounted on cleaned polytetrafluoroethylene sample holders to be analyzed by means of X-ray Fluorescence (XRF) using synchrotron radiation.

2.2. Samples From Potential Source Areas

To depict a coherent geochemical history of the dust deposited at TD, samples collected from potential source areas (PSA) were also considered. It was possible to retrieve data from literature concerning the composition of Antarctic (Baccolo et al., 2014), Australian (Marino et al., 2008), and South American (Gaiero et al., 2008; Smedley et al., 2005) PSA. South Africa was discarded because of its exclusion as a candidate dust source for Antarctica based on previous works (Albani, Mahowald, et al., 2012; Delmonte, Basile-Doelsch, et al., 2004; F. Li et al., 2008). Given the importance of volcanic deposition in Victoria Land (Delmonte et al., 2013), also visible tephra layer observed along TALDICE and related to local Antarctic eruptions were taken into account (Narcisi et al., 2012, 2016).

Additional data about PSA were gathered analyzing 35 further samples. Samples from Antarctica (16) are from ice-free sites of Victoria Land (Delmonte, Baroni, et al., 2010). They mainly consist of regolith produced through both physical (cryoclastism) and chemical weathering. Other samples are glacial deposits and dust collected from natural eolian sediment traps (Delmonte, Baroni, et al., 2010). Australian samples (15 samples) were considered because in addition to being considered the most promising dust source for inner EAIS during the Holocene (Marino et al., 2008; Revel-Rolland et al., 2006), Australia is also the most active source in the Southern Hemisphere in modern times (Prospero et al., 2002). These samples are extensively described by Revel-Rolland et al. (2006). They were collected from the drainage basins of Lake Eyre and Murray-Darling riverine systems, the most important sources of dust in Southern Australia and consist of eolian deposits, riverine sediments, and sand dunes. Concerning South America, the most important dust source for Antarctica during glacial periods (Delmonte et al., 2008), four samples from its southern region were analyzed, expanding the rich literature data set. They are loess-like deposits (deposited during LGM and early Holocene) and sediments of glacial and riverine origin; details can be found in Delmonte, Basile-Doelsch, et al. (2004).

Only the dust fraction below 5-μm diameter—selected following a gravimetric wet method (Delmonte, Basile-Doelsch, et al., 2004)—was considered, so as to make PSA samples comparable to Antarctic ice core dust, where dust spans from submicron dimensions to 5–10 μm (Delmonte, Petit, et al., 2004). In the case of two samples from South America the $<$63-μm fraction was extracted. PSA samples were prepared diluting a given amount of dust in high-purity water and filtering it on a membrane.

2.3. Techniques

2.3.1. Coulter Counter

Dust concentration and particle size were analyzed through Coulter counter (Delmonte et al., 2002; Ruth et al., 2008). A Beckman Coulter Multisizer 4 was used. It was equipped with a 30-μm orifice tube allowing high spectral resolution measurements (400 channels) of particles with a dimeter (spherical equivalent) between 0.6 and 18 μm. About 500 ice samples were measured, complementing the previously published TD dust record (Albani, Delmonte, et al., 2012). Each sample was measured 3 times (0.5 ml for each run). Standard deviations vary between 5% and 10%. Blank signal represented few percentage points of the sample signal, being the average signal to noise ratio 40. The temporal resolution of the updated record is 25 years for the Holocene and the deglaciation (0.7–18 kyr BP) and 70 years for the LGM (18–25 kyr BP). To the aims of the present work two metrics related to the results from Coulter counter were used: CLPP and the FPP. They correspond to coarse local particle percentage and fine particle percentage, respectively, the ratio between the 5–10 μm and the 0.6–10 μm particle flux, and the ratio between the finest particles (0.6–2 μm) and the 0.6–5-μm interval.

2.3.2. Synchrotron Radiation-Based XRF

Major element composition of dust was determined through synchrotron radiation X-ray fluorescence (SR-XRF). Preliminary measurements were carried out at SSRL (Stanford) and successively at the B18 X-ray absorption beamline of the Diamond light source (Dent et al., 2009). To protect samples from the open environment, at Diamond a clean glove box was installed on the beamline, in connection with the experimental chamber. Clean plastic sheets were applied on the inner walls of the chamber to limit the inelastic

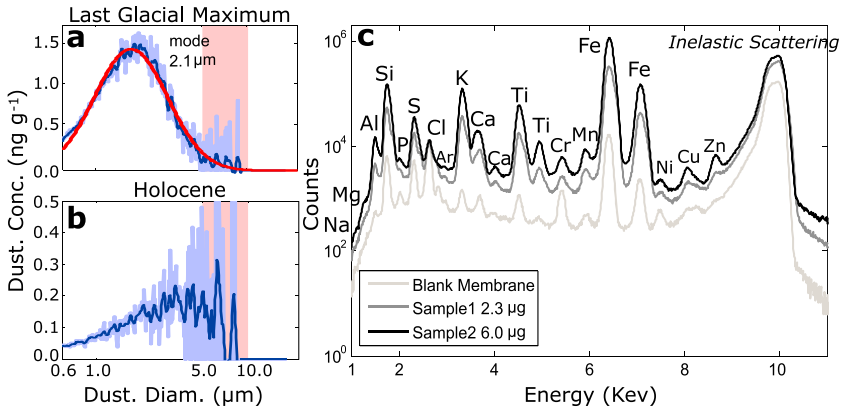

Figure 2. Representative analytical results. (a, b) On the left are two grain size distributions of the particles found in TALDICE determined through coulter counter (different *y* axis scales). The upper graph shows the distribution of a typical sample from Last Glacial Maximum, the lower one from the Holocene. Red area highlights the particles between 5 and 10 μm. For the glacial sample a log-normal fit is superimposed (red curve). (c) On the right are SR-XRF spectra: One is referred to a blank membrane (light gray), the dark gray and black spectra correspond to samples of dust from TALDICE consisting, respectively, of 2.3 and 6.0 μg of dust. TALDICE = TALos Dome Ice CorE; SR-XRF = synchrotron radiation X-ray fluorescence.

scattering resulting from the interaction between the beam and the metallic walls. Fluorescence radiation was induced by a 10-keV beam, and spectra were acquired for 600 s. The energy was selected to measure all major elements, from Na to Fe, (see Figure 2c). The beam was defocused as much as possible, so as to illuminate the largest part of the samples. High vacuum conditions were maintained to remove the contribution from atmospheric gases and to allow the detection of soft X-rays associated to the lighter elements (Kulkarni et al., 2011). A silicon drift detector with a spectral resolution of 140 eV full width at half maximum at the 5.9-KeV Mn Kα line acquired the spectra. They were analyzed using the PyMca software (Solè et al., 2007) and the xraylib data set (Brunetti et al., 2004). An average sample to background ratio of 100 was obtained; further details about the procedure are given in Cibin et al. (2008) and in Marcelli et al. (2012).

Seventy-one samples were measured (36 from TALDICE and 35 from PSA), with the addition of blanks and standards (SRM NIST 2709a, soil reference). SRM were prepared as ice core dust (few microgram of dust deposited on the membranes). Accuracy was evaluated through repeated measurements of SRM. It decreased from light to heavy elements. In the case of Na the standard deviation of the replicates was 25%, but it decreased to 10% for Fe. Recoveries were calculated to assess precision. It ranged from 85% to 115% except for Ca and Na which presented higher differences (133% and 129%, respectively). For such challenging samples (a few microgram of dust) these performances are fully satisfactory. All major elements (Na, Mg, Al, Si, K, Ca, Ti, Mn, and Fe) were quantified, and data were converted in oxides and closed to 100%, since major oxides represent more than 99% of the average upper continental crust composition (Hawkesworth & Kemp, 2006).

2.4. The Chemical Index of Alteration

Two tools were applied to characterize the samples: the chemical index of alteration (CIA) and A-CN-K (Aluminum-Calcium Sodium-Potassium) ternary diagrams. CIA is the relative amount of Al oxide with respect to Al-Ca-Na-K oxides (Nesbitt & Young, 1982). The higher ~~is~~ the CIA, the stronger is weathering since among the considered oxides Al_2O_3 is the only one assumed to be immobile and poorly impacted by chemical alteration. On the contrary Ca, Na, and K are labile and easily removed from the parental material. A-CN-K diagrams are derived from CIA, where it represents the vertical axes. Both tools were originally developed to study the chemical weathering of rocks in relation to past climate (Nesbitt & Young, 1982). But they were also used for provenance studies, in particular, when the potential sources are subjected to different climatic regimes (Bahlburg & Dobrzinski, 2011; C. Li & Yang, 2010). Ice core dust demonstrated to be an interesting field for their application (Marino et al., 2008, 2009).

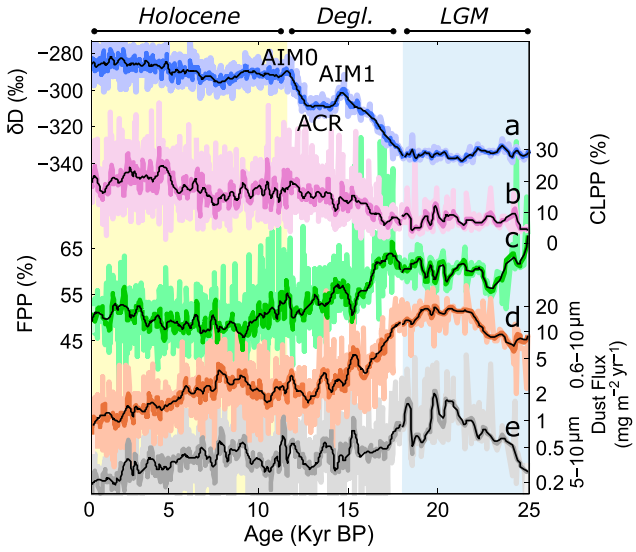

Figure 3. The TALDICE dust record of the last 25 kyr. Variables are presented with three different color shades. The lightest ones refer to raw data, the darker shades are related to smoothed profiles. A first filter was applied to exclude anomalous data as volcanic eruptions or contaminated samples. To this aim we used a LOWESS smoothing algorithm (100-year window for the 0.7–18 kyr time interval, 350 year for the 18–25 kyr one) that excluded samples above or below the interval determined by 6 standard deviations. To highlight structured oscillations, a further filter (black curve) was applied: A Savitsky-Golay filter with a temporal window of 600 year and a third-degree polynomial fitting function. Records show (a) δD, a proxy for temperature (Stenni et al., 2011); (b) CLPP (coarse local particle percentage); (c) FPP (fine particle percentage); (d) total dust flux (0.6–10 μm); and (e) coarse dust flux (5–10 μm). Important climatic events are outlined: ACR (Antarctic cold reversal) and the two Antarctic isotopic maxima (AIM) occurring in the considered time interval. TALDICE = TALos Dome Ice CorE.

3. Results and Discussion

3.1. The TALDICE Dust Record

Figure 3 shows the TD dust record of the last 25 kyr. Dust concentration is converted into deposition flux considering the snow accumulation rate inferred from the chronology (Veres et al., 2013). The general overview of the depositional record at TD resembles that observed in inner EAIS: high dust deposition rates during the LGM, between 25 and 18 kyr B.P., and lower ones during the Holocene (11.7–0.7 kyr B.P.). Considering the size interval between 0.6 and 10 μm, in the LGM up to 20 mg·m^{-2}·year^{-1} of mineral dust were deposited at TD (average 11.9 mg·m^{-2}·year^{-1}), while in the Holocene the flux diminishes, reaching a mean of 2 mg·m^{-2}·year^{-1}. The lowering does not occur in a single step. As everywhere in Antarctica, the first major decrease takes place at the end of LGM, and typical Holocene levels are reached by 12 kyr B.P. But the same Holocene shows a decreasing trend from 7 kyr B.P. to 0.7 kyr B.P., when the dust flux diminishes to less than 1 mg·m^{-2}·yr^{-1}, in agreement with previous estimates of the modern preindustrial flux at the site (Delmonte et al., 2013). If Holocene and LGM are considered as a whole, the ratio between glacial and interglacial dust deposition is 5.7.

Not only the amount of dust deposited at TD varies in response to the glacial/interglacial shift but also its grain size properties. It can be appreciated in Figures 3b and 3c, where the CLPP and FPP metrics are shown. They are related to the relative abundance of coarse particles (5–10 μm, CLPP) and of fine ones (0.6–2 μm). Both are sensitive to glacial/interglacial oscillations. FPP is high during the LGM (average 61%) and lower in the Holocene (50%), CLPP is low in the LGM (7.8%) and higher during the Holocene (19%). The variation rate of the two parameters is also different. FPP decreases sharply with the onset of the deglaciation after 18 kyr B.P. By the beginning of the Holocene (11.7 kyr B.P.) it becomes relatively stable, with a slight increase after 5 kyr B.P. On the contrary, CLPP starts increasing at 18 kyr B.P., but the trend does not stop until the end of the record at 0.7 kyr B.P.

All these pieces of information show that the glacial/interglacial transition deeply impacted the dust cycle at TD, in accordance to what is observed in other Antarctic areas. The drop of dust deposition and of FPP after the LGM are indicative of the reduced activity of the remote dust sources of the Southern Hemisphere as a consequence of the environmental and atmospheric changes that affected the Southern Hemisphere (Lamy et al., 2014; Martìnez-Garcia et al., 2011). Indeed, high FPP suggests a major contribution from remote dust sources, since the longer the atmospheric transport, the more efficient is the removal of coarse particles. Among the many factors, the influence of climate changes on the South American dust sources and the reactivation of the hydrological cycle are assumed to be the most relevant (Kaiser & Lamy, 2010; Sugden et al., 2009).

A South American provenance was attributed to dust in EAIS in a number of studies during the LGM (Basile et al., 1997; Delmonte, Basile-Doelsch, et al., 2004; Delmonte, Petit, et al., 2004), while a different source mixing was observed in the Holocene at Dome C and Vostok (Delmonte et al., 2007; Marino et al., 2008). At TD radiogenic isotopes could not allow to unequivocally identify the dominant source after the LGM (Delmonte et al., 2013), but grain size features suggest that local sources gained importance. This is mostly revealed by CLPP. Given the absence of particles larger than 5 μm in inner EAIS, CLPP characterizes only TD. Their presence concerns both LGM and Holocene, but it become more relevant in the Holocene, with the CLPP increasing from less than 10% to about 20%. The deposition of coarse particles at TD was interpreted as a consequence of the influence played by local Antarctic sources (Albani, Delmonte, et al., 2012), since the shorter the atmospheric transport, the coarser the particles (Tegen & Fung, 1994). The drop of FPP and the rise of CLPP after the LGM at TD (Figure 3c) are related to the suppression of the long-range

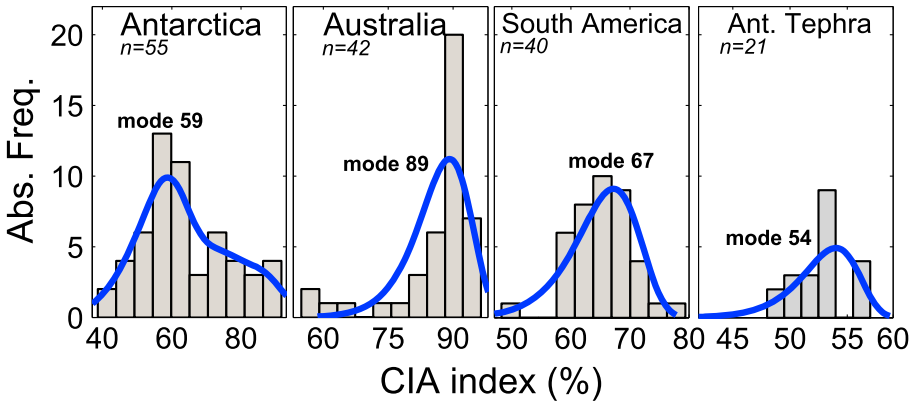

Figure 4. Frequency distribution of the CIA index among the PSA geographical areas considered in this work. Data are from this study and from additional sources (Baccolo et al., 2014; Gaiero et al., 2008; Marino et al., 2008; Narcisi et al., 2012; Smedley et al., 2005). The Weibull distribution was used to fit data and outline modal values. CIA = chemical index of alteration; PSA = potential source areas.

dust transport from South America and to the increased relative importance of local sources. The two size distributions shown in Figure 2 summarize this scenario. LGM dust particles are well described by a log-normal distribution and present fine-modal values (around 2 μm), in accordance to a long-range transport from South America, similar to Dome C (DC; Delmonte, Petit, et al., 2004). Holocene dust conversely shows poor size selection and relatively higher abundance of particles larger than 5 μm, reflecting a more local transport.

3.2. Geochemistry of the Potential Source Areas

The CIA index of ice core samples is compared to that of PSA samples in Figure 4, while A-CN-K diagrams are shown in Figure 5. Australian samples are characterized by a well-defined signature. Their CIA is the highest among the considered samples, with a mean value of 86 ± 7 (standard deviation), confirming the strong chemical alteration that affects Australian sediments and soils (Chittleborough, 1991; Kamber et al., 2005). In the A-CN-K diagram Australian samples occupy the upper apex (Figure 5e), corresponding to Al-rich minerals. Such minerals are associated with intense and prolonged chemical weathering: they are typical in tropical

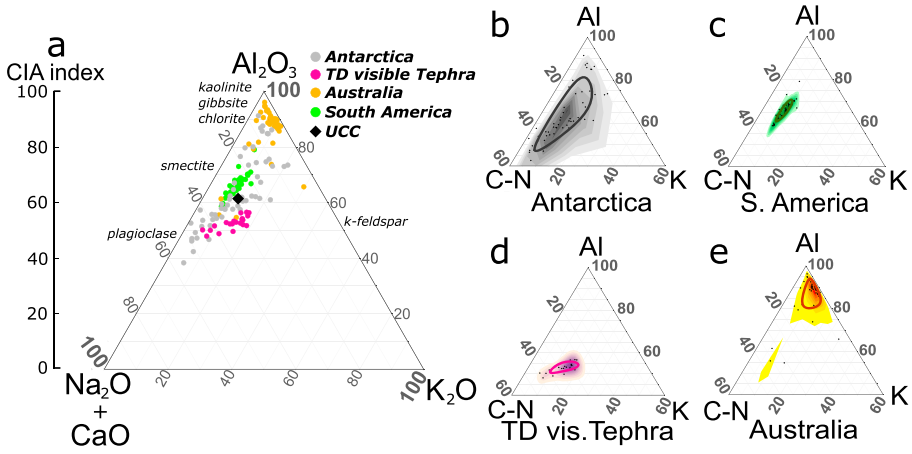

Figure 5. Potential source areas displayed in the A-CN-K diagram. The extended plot (a) presents punctual data, the smaller ones (b–e) are dedicated to the single source areas. In the latter case samples are shown using two-dimensional kernel probability density functions. Contours correspond to 50% confidence intervals. They were calculated as two-dimensional confidence intervals defined by the Mahalanobis distance. Upper continental crust (UCC) reference (Rudnick & Gao, 2003) is reported for comparison as a black diamond. The figure shows the same data as presented in Figure 4. A-CN-K = Aluminum-Calcium Sodium-Potassium; CIA = chemical index of alteration.

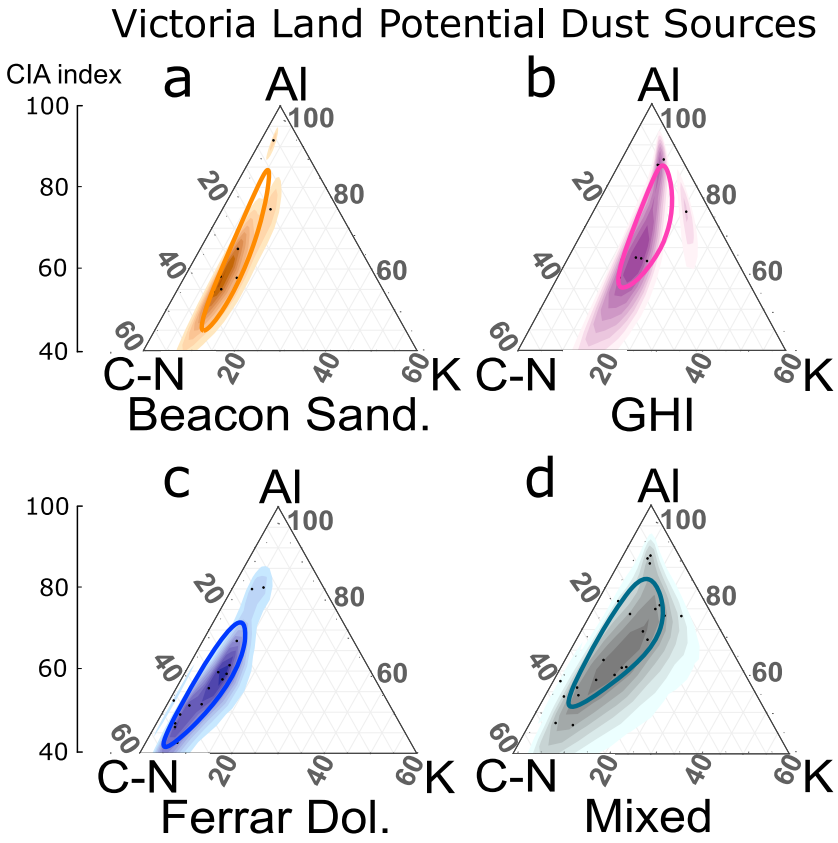

Figure 6. A focus on the Antarctic potential source areas of Victoria land. They are distinguished on the basis of the main lithology of the parental rocks that generated them. When such identification was not possible samples were classified as *mixed*. Extended names: Beacon sandstone, Granite Harbor intrusive, Ferrar dolerite, mixed composition samples. Displayed data were partly published before (Baccolo et al., 2014).

and subtropical regions (Singer, 1980). South American and Antarctic samples present a lower CIA, similar to the upper continental crust reference, thus indicating fresh rocks not yet affected by relevant weathering. This is in accordance with the climate of these regions where chemical alteration is less favored if compared to Australia. Although their average CIA values are similar: 65 ± 5 and 63 ± 9, differences arise in the CIA modal values (67 for South America and 59 for Antarctica). Such evidence is coherent with the colder and drier Antarctic climate. Samples from the two regions share a similar composition, with a substantial overlapping of the associated areas (compare Figures 5b and 5c). It is not unexpected given the geologic history of the two regions, where volcanic activity played a relevant role. What makes them different is variability. South America shows a rather uniform composition (Gaiero et al., 2008). On the contrary, Antarctic PSA span a larger field in the diagram, although all of them were collected in the Victoria Land.

Antarctic samples present the highest CIA excursion, from 40 to 90. The variability is somewhat unexpected. Antarctic climate should limit chemical weathering and thus the occurrence of high CIA. This line of reasoning is supported by the low (below 60) CIA modal value of Antarctic sources, corresponding to fresh rocks (Nesbitt & Young, 1982). To explain the occurrence of high CIA, it should be kept in mind that the Victoria Land sector of the Transantarctic mountains presents a complex geology (Faure & Mensing, 2010), with several ice-free sites that have been exposed since very long periods of time, in the order of million years (Di Nicola et al., 2009, 2012; Oberholzer et al., 2008). Antarctic PSA are punctual sites emerging from the ice with a limited and discontinuous extension. Under such conditions dust mixing processes are unlikely and it is not possible to identify PSA, which can be assumed as representative of a wider area. A similar context favors the emission of heterogeneous dust, where the signature of single outcrops is preserved. This is highlighted in Figure 6, where Antarctic PSA are distinguished according to the lithology of the parental rocks, which are assumed to have produced them. Our results show that different lithological

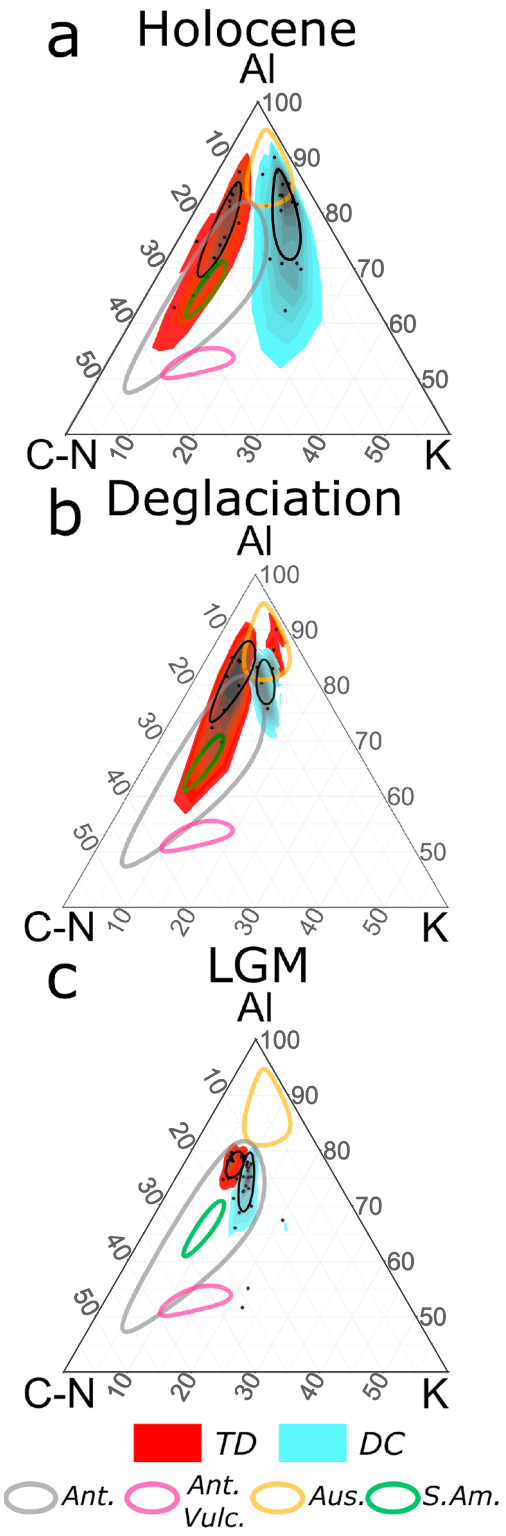

Figure 7. A-CN-K diagrams for the dust extracted from TD and DC ice cores; DC data from Marino et al. (2008, 2009). Samples are presented following the procedure adopted in Figure 5; in addition, the 50% confidence envelops concerning potential source areas are reported. The deglaciation is intended as the time interval between the end of the Last Glacial Maximum (18 kyr BP) and the beginning of the Holocene (11.7 kyr BP). A-CN-K = Aluminum-Calcium Sodium-Potassium; TD = Talos Dome; DC = Dome C.

associations determine different signatures of the dust sources in the A-CN-K diagram. The most evident diversity concerns Ferrar dolerite and Granite Harbor Intrusive (GHI). Given their opposite geochemical composition (basalt vs. granite), they can be considered the end-members characterizing Victoria Land. Dust produced from dolerite outcrops presents low K concentration, in agreement with its basaltic origin. On the contrary, dust and sediments derived from GHI rocks are more potassic, in accordance to the granitic lithology of the GHI association. Moreover, the latter samples present the higher CIA among Antarctic PSA, with values near 90. They are indeed responsible for the secondary peak observed in the CIA frequency distribution (Figure 4a). The reason for that is mostly related to the low concentration of Ca and Na oxides in granite samples. Their removal was already noted as a dominant process in granite weathering (White et al., 1999).

Another important factor related to the occurrence of high CIA values for Antarctic PSA, is the occasional occurrence of favorable conditions for chemical weathering. Ferrar dolerite when exposed to intense solar radiation during austral summer can reach temperatures well above 0°, allowing for the presence of liquid water (Delmonte, Baroni, et al., 2010). This is related to the dark color of the rock and can provide localized spots for chemical weathering, despite the typically unfavorable conditions of Antarctica (Claridge & Campbell, 1984; Hall et al., 2002). Many Victoria Land ice-free sites display extremely old exposure ages, exceeding one million years. Such a long-exposure history, testified by very strong fretted and deeply weathered relict surfaces (Figures 1c and 1d), is surely involved in the alteration process (Di Nicola et al., 2009, 2012; Oberholzer et al., 2008).

A different signature characterizes Antarctic tephra (Figure 5d). They present a uniform composition with CIA below 60. The spread of volcanic material across Victoria Land during the Holocene is mainly related to the activity of a single volcanic district, that is Mount Melbourne, hence the compositional uniformity (Narcisi et al., 2012). The geochemical distinction of local Antarctic tephra from local PSA is a relevant result. Previous attempts to disentangle the crustal and volcanic fractions characterizing Victoria Land dust were not successful (Delmonte et al., 2013).

South American and most Antarctic PSA are aligned on a preferential direction (A-CN). A similar behavior is observed in worldwide riverine sediments. It was related to the dominance of Ca and Na removal in the early phases of alteration within the weathering processes (C. Li & Yang, 2010). On the contrary, highly weathered sediments are easily distributed along the A-K direction, suggesting that the removal of potassium is relevant only after an almost complete removal of Na and Ca (C. Li & Yang, 2010). This is in agreement with the Australian PSA, whose probability distribution in the ternary diagram presents an elongation along this direction.

3.3. Geochemistry of the Atmospheric Dust From the Talos Dome Ice Core

Figure 7 reports A-CN-K diagrams for the TD dust samples. During the Holocene, TD samples are compatible with a local signature, but besides the bare composition, both TD Holocene samples and Antarctic PSA display an elongation along the A-CN axes. The similarity is more pronounced when considering mixed and doleritic Antarctic PSA; on the contrary, the

low concentration of K oxide in TD samples rules out granitic PSA of Victoria Land as significant dust sources (compare Figures 6 and 7). To interpret this finding, it is necessary to consider the geological and geomorphological setting of Victoria Land ice-free sites. Ferrar dolerite and GHI granite are the most common rocks constituting the nunataks of the area near TD (Baroni et al., 2004; Faure & Mensing, 2010; Pour et al., 2018). To explain the prevailing doleritic signature of TD Holocene dust, it is necessary to involve something that favors the transport of doleritic dust and hampers the diffusion of the granitic one. Geomorphology could help in understanding this point, as it can be seen in Figures 1c and 1d. The doleritic outcrops of Victoria Land usually culminate with tabular ice-free plateaus, consisting of high-altitude (2,500–3,000 m) relict flat structural surfaces (Baroni et al., 2004).

Such extended and elevated surfaces are characterized by an intense weathering that allows to produce fine mineral material promptly deflated by winds and injected in the middle troposphere. The morphology of granitic nunataks is completely different and less prone to produce fine materials. They present a typical alpine structure, with pronounced peaks and steep cliffs. The complex and articulate topography favors the accumulation of snowdrift glacierets avoiding the formation of large weathering surfaces as in the previous case. On the contrary, it enhances the development of localized alteration spots (tafoni on rockwalls and weathering pits on flat and gently sloped surfaces) and the accumulation of the resulting sandy regolith at the bottom of the walls, where the slope is lower and deflation is disadvantaged.

The hypothesis of a dominant local source for the dust deposited at TD under interglacial conditions is strengthened. CIA and A-CN-K diagrams distinguish volcanic events from the dust emitted by local PSA (compare Figures 5b and 5d). The same could not be unequivocally deduced from radiogenic isotopes, which could not separate Ferrar dolerite from local tephra (Delmonte et al., 2013). Even if present, the Antarctic volcanic contribute to the Holocene dust budget at TD is secondary and the Sr-Nd signature has to be related to local dust associated to Ferrar dolerite outcrops. During the deglaciation the dust composition at TD is not so different from that of the Holocene, but the area defined by the samples is smaller, and early compositional changes are observed, revealing a trend which is fully expressed in the LGM. Al content remains stable, Na and Ca decrease and K increases. Moreover, in the LGM TD, dust shows a reduced compositional heterogeneity and its distance from South American sources decreases. The overlap between South American and Antarctic sources does not allow to distinguish the two contributes, but the increased geochemical uniformity, Sr-Nd Isotopic results (Delmonte, Andersson, et al., 2010) and grain size distributions (Albani, Delmonte, et al., 2012), point to a dominant South American source during the LGM.

Despite that multiple lines of evidence indicate the Antarctic and South America as the main dust sources at TD during the Holocene and LGM, respectively, differences are observed between TD and the candidate PSA. TD samples present higher CIA values than those of South America and Antarctica, in particular, during the Holocene, when TD samples present an average CIA of 77 ± 8 and Antarctic PSA have a mean value of 63 ± 9. The discrepancy could be related to the contribution of an additional highly weathered source. The only one that satisfies this requirement is Australia. The latter is considered the most important dust source for inner EAIS during the Holocene (Marino et al., 2008; Revel-Rolland et al., 2006). It is thus reasonable to hypothesize that in the Holocene its influence, despite being secondary with respect to local sources, is extended also at TD. But since TD samples show a higher CIA also in the LGM if compared to South American sources, another factor could be involved: atmospheric transport. When mineral dust is transported in the atmosphere, particles are subject to condensation-evaporation cycles, scavenging, photochemical, and acid-base reactions, enhancing the dissolution of soluble and labile mineral fractions (Formenti et al., 2011). The net effect on dust composition is the relative increase of the more stable species, with a rise of CIA.

3.4. A Comparison With Inner East Antarctica

The natural counterpart for understanding and framing the dust cycle in the Ross Sea area is inner EAIS, where local contributes to the dust budget are excluded (Delmonte et al., 2013). This is in line with considerations related to the distance between DC and the Antarctic sources and the setting of the atmospheric circulation in inner Antarctica, which prevents the transport of Antarctic dust from coastal areas toward the interior (Ball, 1956; Parish & Bromwhic, 1987; Wauben et al., 1997). The atmospheric mineral dust deposited in inner EAIS has a remote origin during both glacial and interglacial stages, as revealed by compositional and grain size evidences (Basile et al., 1997; Delmonte, Basile-Doelsch, et al., 2004; Delmonte, Petit, et al., 2004; Revel-Rolland et al., 2006).

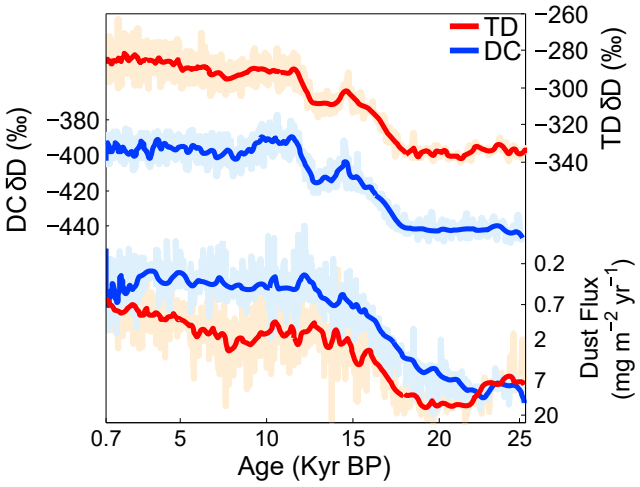

Figure 8. Comparison of the TD and DC water isotope (upper curves) and dust records (lower ones, *y*-scale inverted) over the last 25 kyr. Isotopic data are from Stenni et al. (2004, 2011); part of dust data are from Albani, Delmonte, et al. (2012) and Lambert et al. (2008). Light shades refer to raw data, darker ones to smoothed data. TD = Talos Dome; DC = Dome C.

At TD this description fits only for the LGM, whereas the Holocene is different. A first element shared by TD and DC in the LGM is dust flux magnitude: both range between 10 and 15 mg·m^{-2}·year^{-1} (Figure 8). In addition, they share similar grain size features, with well-sorted distributions and fine-modal values (Albani, Delmonte, et al., 2012). Our major element data show that also the geochemical composition is quite similar in this period (Figure 7c), as confirmed by Sr-Nd isotopes (Delmonte, Andersson, et al., 2010). These pieces of information point to a uniform South American source on EAIS during glacials, owing to the coupling that characterizes Antarctic climate and South America sources (Lambert et al., 2008).

A different picture is found after the LGM. The dust records of DC and TD diverge in terms of dust flux and of dust composition around 22 kyr B.P., just before the deglaciation. At the end of LGM, DC dust deposition starts decreasing, as a consequence of the reduced activity of South American sources, extremely sensitive to climate changes (Albani, Mahowald, et al., 2012; Mahowald et al., 1999). At TD the decline is slower, younger, and more irregular, with episodes of enhanced deposition. TD dust flux remains higher throughout the Holocene, if compared to DC (Figure 8). Indeed, Holocene mean dust deposition at DC is 0.4 mg·m^{-2}·year^{-1}, while at TD it is 2.1 mg·m^{-2}·year^{-1}, about 5 times higher. The gap is explained taking into account the influence of local Antarctic sources. Their activity is not limited to the Holocene, since mineral particles exceeding 5 μm (assumed to be exclusively local) are deposited at TD during both Holocene and LGM, with only a weak increase during LGM (Figure 3e). What really changes is the relative contribution of remote and local sources. While the absolute depositional flux of coarse local particles at TD is quite stable in the last 25 kyr (Figure 3e), the relative one is not, as demonstrated by CLPP. It increases from a mean of 7.8% in the LGM, to 19% in the Holocene (Figure 3b), showing that local sources progressively gain importance. Concurrently the FPP (related to very fine particles, i.e., remote ones) decreases (Figure 3c). These data suggest that in the TD area the transition to interglacial conditions had a double effect on the dust cycle. On the one side, it determined the reduction of dust deposition from remote sources; on the other side, it resulted in an increased role of local Antarctic sources with respect to the regional context. The same conclusions can be drawn directly comparing TD and DC records and assuming the latter as a reference for remote dust deposition in EAIS. As it is reassumed in Table 1, during LGM the local dust accounts for 28% of total deposition at TD; on the contrary, during the Holocene it accounts for more than 80%, revealing that local sources of Victoria Land not only become prevalent but completely dominant in this area. But the local flux is not constant; indeed, a decreasing trend is observed after 7–8 kyr B.P. (Figure 8). We explain it as a consequence of the exhaustion of local sources across the Holocene. The weak increase of FPP and CLPP after 5 kyr B.P. supports this hypothesis. It is expected that more exhaust dust sources become progressively enriched in coarse particles, since the finer ones are promptly mobilized in the atmosphere. At the same time the reduction of the local dust flux is responsible for a relative increase of the flux associated to the weak remote sources, as supported by the slight increase of FPP.

Table 1
A Summary of the Dust Depositional Fluxes Observed at TD and DC in the Holocene and in the LGM

	Talos dome dust flux				Dome C dust flux			
	Holocene		LGM		Holocene		LGM	
Climatic period	(mg·m^{-2}·year^{-1})	%	(mg·m^{-2}·year^{-1})	(%)	(mg·m^{-2}·year^{-1})	(%)	(mg·m^{-2}·year^{-1})	(%)
Remote contribute	0.4 ± 0.3	19	8.6 ± 2.3	72	0.4 ± 0.3	100	8.6 ± 2.3	100
Local contribute	1.7 ± 1.9	81	3.3 ± 7.7	28	0	0	0	0

Note. For each period absolute and relative (%) contributes from remote and local sources were estimated, assuming the DC record as the reference for the deposition related to the activity of extra-Antarctic remote sources. Standard deviations calculated for the different periods are reported. TD = Talos Dome; DC = Dome C; LGM = Last Glacial Maximum.

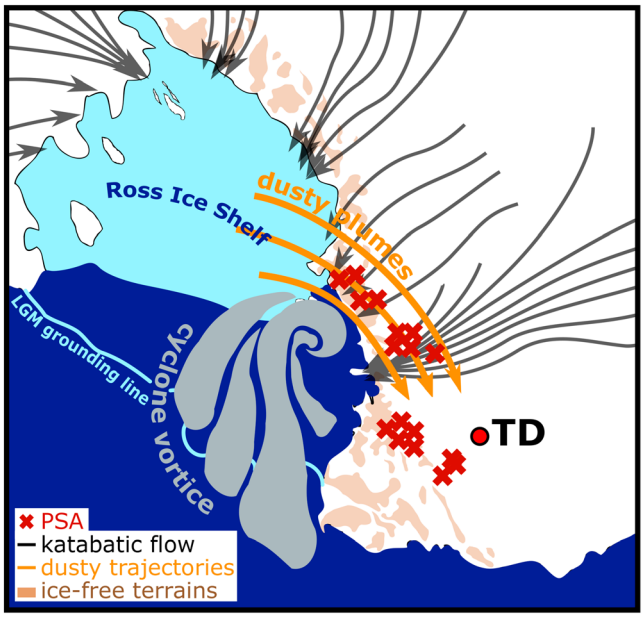

Figure 9. A conceptual scheme representing the atmospheric setting associated to the transport of local dust from Victoria land to Talos dome in the Holocene. Black arrows refer to the mean katabatic wind field (Parish & Bromwhic, 1987). The position and the structure of the cyclone reflect a typical synoptic scenario related to such contexts (Bromwhic, 1991). Trajectories responsible for the transport of dust from the Victoria land toward TD, triggered by local cyclones, are inspired by modern back trajectories reanalyses (Delmonte et al., 2013). Ice-free terrains are the elevated areas where the occurrence of ice-free sites is more frequent. They correspond to the Transantarctic Mountains. LGM Ross shelf grounding line was taken from Spector et al. (2017). TD = Talos Dome; LGM = Last Glacial Maximum; PSA = potential source areas.

The regionalization of the dust cycle in the Ross Sea area, already noted in earlier studies (Albani, Delmonte, et al., 2012; Delmonte, Baroni, et al., 2010), is now also supported by geochemical data (Figure 7) and can be interpreted in terms of atmospheric and climatic changes that occurred in the region. The retreat of the Ross Sea ice shelf after the deglaciation allowed a deeper penetration of Ross Sea mesoscale cyclones toward the Antarctic interior (Carrasco et al., 2003; Delmonte et al., 2013). Modern back trajectories reanalysis shows that this situation is favorable to the transport of dust from high-elevation ice-free areas of Victoria Land toward the Talos Dome area (Delmonte et al., 2013; Scarchilli et al., 2011). A conceptual scheme is presented in Figure 9.

The disruption of the dust-climate coupling between Antarctica and South America during the Holocene and likely earlier interglacials, leads to different dynamics in inner EAIS. In general, the influx of dust transported from remote dry areas of the Southern Hemisphere to Antarctica dropped to extremely low values (below 0.5 $mg \cdot m^{-2} \cdot year^{-1}$). In the case of DC and inner EAIS, grain size (Delmonte, Petit, et al., 2004) and geochemical constraints (Marino et al., 2008; Revel-Rolland et al., 2006) show that the Holocene source for the dust is likely extra-Antarctic also during the Holocene, with a significant contribution from Australia, as it is shown in Figure 7c. Australia is the most important dust source in the Southern Hemisphere at present (Prospero et al., 2002), and its activity was not influenced by climate changes in the late Pleistocene as much as in the case of Southern South America sources (Hesse & McTainsh, 2003). Finding an Australian signature in inner EAIS is not unexpected. The polar vortex, centered on the middle of EAIS (Kakegawa et al., 1986), enhances the convergence of air masses from lower latitudes via high tropospheric pathways. Inner EAIS can be thus considered as a sampler for the background dust of the Southern Hemisphere, which during interglacial periods is dominated by Australian dust. In addition, models identify high tropospheric pathways as the dominant ones allowing for the transport of Australian dust to EAIS (Krinner et al., 2010; F. Li et al., 2008).

4. Conclusions

The Talos Dome ice core is used to reconstruct the dust cycle in a peripheral sector of the EAIS over the last 25 kyr. The shift from glacial to interglacial conditions has a deep impact on the dust depositional regime of the Ross Sea area, but it is different with respect to what was observed in inner East Antarctica. A comparison with DC confirms that during glacial periods the dust cycle of the entire East Antarctica is well coupled to the emission activity of lower-latitude dust sources, suggesting a pan-Antarctic scenario during cold climatic phases. On the contrary, under interglacial conditions, the connection between high and lower latitudes tend to fade, inducing a drastic reduction of dust deposition from remote sources and allowing local dynamics gaining importance. What mainly distinguishes peripheral and inner sites is the influence of local Antarctic sources, located at the margins of ice sheets. Such sources are active during both glacial and interglacial periods, but their importance is relevant in interglacials, when remote dust sources are almost inactive. With the onset of Holocene, the dust cycle at Talos Dome becomes markedly local and more influenced by the local setting of the Ross Sea and Victoria Land areas. Thanks to a short atmospheric transport and to extremely localized dust sources, mixing processes are unfavored, enhancing the emission of dust with a variable composition, reflecting the geological and geomorphological complexity of the region.

Our results show how peripheral Antarctic sites are capable of recording signals that are complementary to the ones preserved by ice cores retrieved from inner sites. This work concerns atmospheric mineral dust, but similar considerations could be easily extended. Only by considering both internal and peripheral records is it

possible to depict a coherent and complete climatic history for Antarctica, in particular, during Holocene, when local climatic variability is more clearly expressed.

Acknowledgments
The Talos Dome Ice core Project (TALDICE), a joint European program, is funded by national contributions from Italy, France, Germany, Switzerland, and the United Kingdom. Primary logistical support was provided by PNRA at Talos Dome. This is TALDICE publication 49. This study has been partially supported by DARA (Dipartimento per gli Affari Regionali e Autonomie of Italian Presidenza del Consiglio dei Ministri) in the framework of the MIAMI (Monitoraggio dell'Inquinamento Atmosferico della Montagna Italiana) project. Synchrotron radiation measurements were carried out in the framework of Proposals 90U5 and 3082M at SSRL, a national user facility operated by Stanford University on behalf of the U.S. Department of Energy, Office of Basic Energy Sciences and at Diamond in the framework of the proposals NT1984. This article is an outcome of Project MIUR-Dipartimenti di Eccellenza 2018–2022. We thank Anders Svensson and Denis-Didier Rousseau for their valuable revision that improved the quality of the present work. Full data are available as supporting information and in the PANGAEA data repository at https://doi.org/10.1594/PANGAEA.890907.

References

Aarons, S., Aciego, S. M., Gabrielli, P., Delmonte, B., Koornneef, J. M., Wegner, A., et al. (2016). The impact of glacier retreat from the Ross Sea on local climate: characterization of mineral dust in the Taylor Dome ice core, East Antarctica. *Earth and Planetary Science Letters*, *444*, 34–44.

Aarons, S. M., Aciego, S. M., Arendt, C. A., Blakowski, M. A., Steigmeyer, A., Gabrielli, P., et al. (2017). Dust composition changes from Taylor Glacier (East Antarctica) during the last glacial-interglacial transition: A multi-proxy approach. *Quaternary Science Reviews*, *162*, 60–71.

Albani, S., Delmonte, B., Maggi, V., Baroni, C., Petit, J. R., Stenni, B., et al. (2012). Interpreting last glacial to Holocene dust changes at Talos Dome (East Antarctica): implications for atmospheric variations from regional to hemispheric scales. *Climate of the Past*, *8*, 741–750.

Albani, S., Mahowald, N., Delmonte, B., Maggi, V., & Winckler, G. (2012). Comparing modeled and observed changes in mineral dust transport and deposition to Antarctica between the Last Glacial Maximum and current climates. *Climate Dynamics*, *38*, 1731–1755.

Albani, S., Mahowald, N. M., Winckler, G., Anderson, R. F., Bradtmiller, L. I., Delmonte, B., et al. (2015). Twelve thousand years of dust: The Holocene global dust cycle constrained by natural archives. *Climate of the Past*, *11*, 869–903.

Baccolo, G., Baroni, C., Clemenza, M., Delmonte, B., Maggi, V., Motta, A., et al. (2014). Neutron activation analysis on sediments from Victoria Land, Antarctica: Multi-elemental characterization of potential atmospheric dust sources. *Journal of Radioanalaytical and Nuclear Chemistry*, *299*, 1615–1623.

Bahlburg, H., & Dobrzinski, N. (2011). A review of the chemical index of alteration (CIA) and its application to the study of Neoproterozoic glacial deposits and climate transitions. In *Memoirs 36 - The Geological Record of Neoproterozoic Glaciations*, (pp. 81–92). London: Geological Society.

Ball, F. K. (1956). The theory of strong katabatic winds. *Australian Journal of Physics*, *9*, 373–386.

Baroni, C., Frezzotti, M., Salvatore, M. C., Meneghel, M., Tabacco, I. E., Vittuari, L., et al. (2004). Antarctic geomorphological and glaciological 1:250 000 map series: Mount Murchison quadrangle, northern Victoria Land. Explanatory notes. *Annals of Glaciology*, *39*, 256–264.

Basile, I., Grousset, F. E., Revel, M., Petit, J. R., Biscaye, P. E., & Barkov, N. I. (1997). Patagonian origin of glacial dust deposited in East Antarctica (Vostok and Dome C) during glacial stages 2, 4 and 6. *Earth and Planetary Science Letters*, *146*, 573–589.

Bertler, N. A., Conway, H., Dahl-Jensen, D., Emanuelsson, D. B., Winstrup, M., Vallelonga, P. T., et al. (2018). The Ross Sea dipole—Temperature, snow accumulation and sea ice variability in the Ross Sea region, Antarctica, over the past 2,700 years. *Climate of the Past*, *14*, 193–214.

Bory, A., Wolff, E., Mulvaney, R., Jagoutz, E., Wegner, A., Ruth, U., et al. (2010). Multiple sources supply eolian mineral dust to the Atlantic sector of coastal Antarctica: Evidence from recent snow layers at the top of Berkner Island ice sheet. *Earth and Planetary Science Letters*, *291*, 138–148.

Bromwhic, D. H. (1991). Mesoscale cyclogenesis over the southwestern Ross Sea linked to strong katabatic winds. *Monthly Weather Review*, *119*, 1736–1752.

Brunetti, A., Sanchez del Rio, M., Golosio, B., Simionovici, A., & Somogyi, A. (2004). A library for X-ray–matter interaction cross sections for X-ray fluorescence applications. *Spectrochimica Acta B*, *59*, 1725–1731.

Carrasco, J. F., Bromwich, D. H., & Monaghan, J. A. (2003). Distribution and characteristics of mesoscale cyclones in the Antarctic: Ross Sea eastward to the Weddell Sea. *Monthly Weather Review*, *131*, 289–301.

Chittleborough, D. J. (1991). Indices of weathering for soils and palaeosols formed on silicate rocks. *Australian Journal of Earth Sciences*, *38*, 115–120.

Cibin, G., Marcelli, A., Maggi, V., Sala, M., Marino, F., Delmonte, B., et al. (2008). First combined total reflection X-ray fluorescence and grazing incidence X-ray absorption spectroscopy characterization of aeolian dust archived in Antarctica and Alpine deep ice cores. *Spectrochimica Acta B*, *63*, 1503–1510.

Claridge, G. G., & Campbell, I. B. (1984). Mineral transformation during the weathering of dolerite under cold arid conditions in Antarctica. *New Zealand Journal of Geology and Geophysics*, *27*, 537–545.

Delmonte, B., Andersson, P. S., Hansson, M., Shoberg, H., Petit, J. R., Basile-Doelsch, I., et al. (2008). Aeolian dust in East Antarctica (EPICA-Dome C and Vostok): provenance during glacial ages over the last 800 kyr. *Geophysical Research Letters*, *35*, L07703. https://doi.org/10.1029/2008GL033382

Delmonte, B., Andersson, P. S., Shoberg, H., Hansson, M., Petit, J. R., Delmas, R., et al. (2010). Geographic provenance of aeolian dust in East Antarctica during Pleistocene glaciations: Preliminary results from Talos Dome and comparison with East Antarctic and new Andean ice core data. *Quaternary Science Reviews*, *29*, 256–264.

Delmonte, B., Baroni, C., Andersson, P. S., Narcisi, B., Salvatore, M. C., Petit, J. R., et al. (2013). Modern and Holocene aeolian dust variability from Talos Dome (Northern Victoria Land) to the interior of the Antarctic ice sheet. *Quaternary Science Reviews*, *64*, 76–89.

Delmonte, B., Baroni, C., Andersson, P. S., Shoberg, H., Hansson, M., Aciego, S., et al. (2010). Aeolian dust in the Talos Dome ice core (East Antarctica, Pacific/Ross Sea sector): Victoria Land versus remote sources over the last two climatic cycle. *Journal of Quaternary Science*, *25*, 1327–1337.

Delmonte, B., Basile-Doelsch, I., Petit, J. R., Maggi, V., Revel-Rolland, M., Michard, A., et al. (2004). Comparing the Epica and Vostok dust record during the last 220,000 years: stratigraphical correlation and provenance in glacial periods. *Earth Science Reviews*, *66*, 63–87.

Delmonte, B., Paleari, C. I., Andò, S., Garzanti, E., Andersson, P. S., Petit, J. R., et al. (2017). Causes of dust size variability in central East Antarctica (Dome B): Atmospheric transport from expanded South American sources during Marine Isotope Stage 2. *Quaternary Science Reviews*, *168*, 55–68.

Delmonte, B., Petit, J. R., Andersen, K. K., Basile-Doelsch, I., Maggi, V., & Lipenkov, Y. A. (2004). Dust size evidence for opposite regional atmospheric circulation changes over east Antarctica during the last climatic transition. *Climate Dynamics*, *23*, 427–438.

Delmonte, B., Petit, J. R., Basile-Doelsch, I., Jagoutz, E., & Maggi, V. (2007). Late quaternary interglacials in East Antarctica from ice-core dust records. In F. Sirocko, T. Litt, & M. Clausen (Eds.), *The Climate of Past Interglacials*, (pp. 53–73). Amsterdam: Elsevier.

Delmonte, B., Petit, J. R., & Maggi, V. (2002). Glacial to Holocene implications of the new 27000-year dust record from the EPICA Dome C (East Atarctica) ice core. *Climate Dynamics*, *18*, 647–660.

Dent, A. J., Cibin, G., Ramos, S., Smith, A. D., Scott, S. M., Varandas, L., et al. (2009). B18: A core XAS spectroscopy beamline for Diamond. *Journal of Physics: Conference Series*, *190*. https://doi.org/10.1088/1742-6596/190/1/012039

Di Nicola, L., Baroni, C., Straski, S., Salvatore, M. C., Schlüchter, C., Akçtar, N., et al. (2012). Multiple cosmogenic nuclides document the stability of the East Antarctic ice sheet in northern Victoria land since the Late Miocene (5e7 Ma). *Quaternary Science Reviews*, *57*, 85–94.

Di Nicola, L., Strasky, S., Schlüchter, C., Salvatore, M. C., Akçar, N., Kubik, P. W., et al. (2009). Multiple cosmogenic nuclides document complex Pleistocene exposure history of glacial drifts in Terra Nova Bay (northern Victoria Land, Antarctica). *Quaternary Research*, *71*, 83–92.
Faure, G., & Mensing, T. M. (2010). *The Transantarctic mountains: Rocks, ice, meteorites and water*. Dordrecht, The Netherlands: Springer.
Formenti, P., Schutz, L., Balkanski, Y., Desboeufs, K., Ebert, M., Kandler, K., et al. (2011). Recent progress in understanding physical and chemical properties of African and Asian mineral dust. *Atmospheric Chemistry and Pysics*, *11*. https://doi.org/10.5194/acp-11-8231-2011
Frezzotti, M., Bitelli, G., De Michelis, P., Deponti, A., Forieri, A., Gandolfi, S., et al. (2004). Geophysical survey at Talos Dome, East Antarctica: The search for a new deep-drilling site. *Annals of Glaciology*, *39*, 423–432.
Gabrielli, P., Barbante, C., Boutron, C., Cozzi, G., Gaspari, V., Planchon, F., et al. (2005). Variations in atmospheric trace elements in Dome C (East Antarctica) ice over the last two climatic cycles. *Atmospheric Environment*, *39*, 6420–6429.
Gabrielli, P., Wegner, A., Petit, J. R., Delmonte, B., De Deckker, P., Gaspari, V., et al. (2010). A major glacial-interglacial change in aeolian dust composition inferred from Rare Earth Elements in Antarctic ice. *Quaternary Science Reviews*, *29*, 265–273.
Gaiero, D. M., Brunet, F., Probst, J. L., & Depetris, P. J. (2008). A uniform isotopic and chemical signature of dust exported from Patagonia: Rock sources and occurence in southern environments. *Chemical Geology*, *238*, 107–120.
Gaudichet, A., De Angelis, M., Joussame, S., Petit, J. R., Korotkevich, Y. S., & Petrov, V. N. (1992). Comments on the origin of dust in East Antarctica for present and ice age conditions. *Journal of Atmospheric Chemistry*, *14*, 129–142.
Hall, K., Thorn, C. E., Matsuoka, N., & Prick, A. (2002). Weathering in cold regions: Some thoughts and perspectives. *Progress in Physical Geography*, *26*, 577–603.
Hawkesworth, J. C., & Kemp, A. I. (2006). Evolution of the continental crust. *Nature*, *443*, 811–817.
Hesse, P. P., & McTainsh, G. H. (2003). Australian dust deposits: Modern processes and quaternary record. *Quaternary Science Reviews*, *22*, 2007–2035.
Jickells, T. D., An, Z. S., Andersen, K. K., Baker, A. R., Bergametti, G., Brooks, N., et al. (2005). Global iron connections between desert dust, ocean biogeochemistry and climate. *Science*, *308*, 67–71.
Kaiser, J., & Lamy, F. (2010). Links between Patagonian ice sheet fluctuations and Antarctic dust variability during the last glacial period (MIS 4–2). *Quaternary Science Reviews*, *29*, 1464–1471.
Kakegawa, H., Yasunari, T., & Kawamura, T. (1986). Seasonal and intra-seasonal fluctuations of polar anticyclone and circumpolar vortex over Antarctica. *Memoirs of National Institute of Polar Research*, *45*, 19–29.
Kamber, B. S., Greig, A., & Collerson, K. D. (2005). A new estimate for the composition of weathered young upper continental crust from alluvial sediments, Queensland, Australia. *Geochimica et Cosmochimica Acta*, *69*, 1041–1058.
Kawamura, K., Abe-Ouchi, A., Motoyama, H., Ageta, Y., Aoki, S., Azuma, N., et al. (2017). State dependence of climatic instability over the past 720,000 years from Antarctic ice cores and climate modeling. *Science Advances*, *3*. https://doi.org/10.1126/sciadv.1600446
Koffman, B. G., Kreutz, K. J., Breton, D. J., Kane, E. J., Winski, D. A., Birkel, S. D., et al. (2014). Centennial-scale variability of the Southern Hemisphere westerly wind belt in the eastern Pacific over the past two millennia. *Climate of the Past*, *10*, 1125–1144.
Krinner, G., Petit, J. R., & Delmonte, B. (2010). Altitude of atmospheric tracer transport towards Antarctica in present and glacial climate. *Quaternary Science Reviews*, *29*, 274–284.
Kulkarni, P., Baron, P. A., & Willeke, K. (2011). *Aerosol measurement: Principles, techniques, and applications*. New Jersey: John Wiley & Sons.
Lambert, F., Delmonte, B., Petit, J. R., Bigler, M., Kaufmann, P. R., Hutterli, M. A., et al. (2008). Dust-climate couplings over the past 800.000 years from the EPICA Dome C ice core. *Nature*, *452*, 616–619.
Lamy, F., Gersonde, R., Winckler, G., Esper, O., Jaeschke, A., Kuhn, G., et al. (2014). Increased dust deposition in the Pacific Southern Ocean during glacial periods. *Science*, *343*, 403–407.
Li, C., & Yang, S. (2010). Is chemical index of alteration (CIA) a reliable proxy for chemical weathering in global drainage basins? *American Journal of Science*, *310*, 111–127.
Li, F., Ginoux, P., & Ramaswamy, V. (2008). Distribution, transport, and deposition of mineral dust in the Southern Ocean and Antarctica: Contribution of major sources. *Journal of Geophysical Research*, *113*, D10207. https://doi.org/10.1029/2007JD009190
Maher, B. A., Prospero, J. M., Mackie, D., Gaiero, D., Hesse, P. P., & Balkanski, Y. (2010). Global connections between aeolian dust, climate and ocean biogeochemistry at the present day and at the Last Glacial Maximum. *Earth Science Reviews*, *99*, 61–97.
Mahowald, N., Albani, S., Engelstaedter, S., Winckler, G., & Goman, M. (2011). Model insight into glacial–interglacial paleodust records. *Quaternary Science Reviews*, *30*, 832–854.
Mahowald, N., Kohfeld, K., Hansson, M., Balkanski, Y., Harrison, S. P., Prentice, I., et al. (1999). Dust sources and deposition during the Last Glacial Maximum and current climate: A comparison of model results with paleodata from ice cores and marine sediments. *Journal of Geophysical Research*, *104*, 15,895–15,916. https://doi.org/10.1029/1999JD900084
Mahowald, N. M., Kloster, S., Engelstaedter, S., Moore, J. K., Mukhopadhyay, S., McConnel, J. R., et al. (2010). Observed 20th century desert dust variability: Impact on climate and biogeochemistry. *Atmospheric Chemistry and Physics*, *10*, 10,875–10,893.
Marcelli, A., Hampai, D., Giannone, F., Sala, M., Maggi, V., Marino, F., et al. (2012). XRF-XANES characterization of deep ice core insoluble dust. *Journal of Analytical Atomic Spectrometry*, *27*, 33–37.
Marcelli, C., & Maggi, V. (2017). *Aerosols in snow and ice. Markers of environmental pollution and climatic changes: European and Asian perspectives*. Roma: Superstripes Press.
Marino, F., Castellano, E., Ceccato, D., De Deckker, P., Delmonte, B., Ghermandi, G., et al. (2008). Defining the geochemical composition of the EPICA Dome C ice core dust during the last glacial-interglacial cycle. *Geochemistry, Geophysics, Geosystems*, *9*, Q10018. https://doi.org/10.1029/2008GC002023
Marino, F., Castellano, E., Nava, S., Chiari, M., Ruth, U., Wegner, A., et al. (2009). Coherent composition of glacial dust on opposite sides of the East Antarctic Plateau inferred from the deep EPICA ice cores. *Geophysical Research Letters*, *36*, L23703. https://doi.org/10.1029/2009GL040732
Martìnez-Garcia, A., Rosell-Melé, A., Jaccard, S. L., Geibert, W., Sigman, D. M., & Haug, G. H. (2011). Southern Ocean dust–climate coupling over the past four million years. *Nature*, *476*, 312–315.
Marx, S. K., Kamber, B. S., McGowan, H. A., Petherick, L. M., McTainsh, G. H., Stromsoe, N., et al. (2018). Palaeo-dust records: A window to understanding past environments. *Global and Planetary Change*, *165*, 13–43.
McConnell, J. R., Aristarain, A. J., Banta, J. R., Edwards, P. R., & Simoes, J. C. (2007). 20th-century doubling in dust archived in an Antarctic Peninsula ice core parallels climate change and desertification in South America. *PNAS*, *104*, 5743–5748.
Mezgec, K., Stenni, B., Crosta, X., Masson-Delmotte, V., Baroni, C., Braida, M., et al. (2017). Holocene sea ice variability driven by wind and polynya efficiency in the Ross Sea. *Nature Communications*, *8*. https://doi.org/10.1038/s41467-017-01455-x
Narcisi, B., Petit, J., Langone, A., & Stenni, B. (2016). A new Eemian record of Antarctic tephra layers retrieved from the Talos Dome ice core (Northern Victoria Land). *Global and Planetary Change*, *137*, 69–78.
Narcisi, B., Petit, J. R., Delmonte, B., Scarchilli, C., & Stenni, B. (2012). A 16,000 yr tephra framework for the Antarctic ice sheet: A contribution from the new Talos Dome core. *Quaternary Science Reviews*, *49*, 52–63.

Neff, P. D., & Bertler, N. A. (2015). Trajectory modeling of modern dust transport to the Southern Ocean. *Journal of Geophysical Research: Atmospheres*, *120*, 9303–9322. https://doi.org/10.1002/2015JD023304

Nesbitt, H. W., & Young, G. M. (1982). Early Proterozoic climates and plate motions from major element chemistry of lutites. *Nature*, *299*, 715–717.

Oberholzer, P., Baroni, C., Salvatore, M. C., Baur, H., & Wieler, R. (2008). Dating late Cenozoic erosional surfaces in Victoria Land, Antarctica, with cosmogenic neon in pyroxenes. *Antarctic Science*, *20*, 89–98.

Parish, T. R., & Bromwhic, D. H. (1987). The surface windfield over the Antarctic ice sheets. *Nature*, *328*, 51–54.

Petit, J. R., & Delmonte, B. (2009). A model for large glacial–interglacial climate-induced changes in dust and sea salt concentrations in deep ice cores (central Antarctica): Palaeoclimatic implications and prospects for refining ice core chronologies. *Tellus B*, *61*, 768–790.

Pour, A. B., Park, Y., Park, T. Y. S., Hong, J. K., Hashim, M., Woo, J., et al. (2018). Regional geology mapping using satellite-based remote sensing approach in Northern Victoria Land, Antarctica. *Polar Science*, *16*, 23–46. https://doi.org/10.1016/j.polar.2018.02.004

Prospero, J. M., Ginoux, P., Torres, O., Nicholson, S. E., & Gill, T. E. (2002). Environmental characterization of global sources of atmospheric soil dust identified with the Nimbus 7 Total Ozone Mapping Spectrometer (TOMS) absorbing aerosol product. *Reviews of Geophysics*, *40*(1), 1002. https://doi.org/10.1029/2000RG000095

Rea, D. K. (1994). The paleoclimatic record provided by eolian deposition in the deep sea: The geologic history of wind. *Reviews of Geophysics*, *32*, 159–195. https://doi.org/10.1029/93RG03257

Revel-Rolland, M., De Deckker, P., Hesse, P. P., Magee, J. W., Basile-Doelsch, I., Grousset, F., et al. (2006). Eastern Australia: A possible source of dust in East Antarctica interglacial ice. *Earth and Planetary Science Letters*, *249*, 1–13.

Ridgwell, A. J., & Watson, A. (2002). Feedback between aeolian dust, climate, and atmospheric CO_2 in glacial time. *Paleoceanography*, *17*(4), 1059. https://doi.org/10.1029/2001PA000729

Rudnick, R. L., & Gao, S. (2003). The composition of continental crust. In H. D. Holland, & K. K. Turekian (Eds.), *Treatise on geochemistry*, (Vol. 3, pp. 1–64). Pergamon, Oxford: Elsevier.

Ruth, U., Barbante, C., Bigler, M., Delmonte, B., Fischer, H., Gabrielli, P., et al. (2008). Proxies and measurement techinques for mineral dust in Antarctic ice cores. *Environmental Science and Technology*, *42*, 5675–5681.

Scarchilli, C., Frezzotti, M., & Ruti, P. M. (2011). Snow precipitation at four ice core sites in East Antarctica: provenance, seasonality and blocking factors. *Climate Dynamics*, *37*, 2107–2125.

Singer, A. (1980). The paleoclimatic interpretation of clay minerals in sediments—A review. *Earth Science Reviews*, *15*, 303–326.

Smedley, P. L., Kinniburgh, D. G., Macdonald, D. M., Nicolli, H. P., Barros, A. J., Tullio, J. O., et al. (2005). Arsenic associations in sediments from the loess acquifer of La Pampa, Argentina. *Applied Geochemistry*, *20*, 989–1016.

Solè, V. A., Papillon, E., Cotte, M., Walter, P., & Susini, J. (2007). A multiplatform code for the analysis of energy-dispersive X-ray fluorescence spectra. *Spectrochimica Acta B*, *62*, 63–68.

Spector, P., Stone, J., Cowdery, S. G., Hall, B., Conway, H., & Bromley, G. (2017). Rapid early-Holocene deglaciation in the Ross Sea, Antarctica. *Geophysical Research Letters*, *44*, 7817–7825. https://doi.org/10.1002/2017GL074216

Stenni, B., Jouzel, J., Masson-Delmotte, V., Torhlisberger, R., Castellano, E., Cattani, O., et al. (2004). A late-glacial high-resolution site and source temperature record derived from the EPICA Dome C isotope records (East Antarctica). *Earth and Planetary Science Letters*, *217*, 183–195.

Stenni, B., Buiron, D., Frezzotti, M., Albani, S., Barbante, C., Bard, E., et al. (2011). Expression of the bipolar see-saw in Antarctic climate record during the last deglaciation. *Nature Geoscience*, *4*, 46–49.

Sugden, D. E., McCulloch, R. D., Bory, A. J., & Hein, A. S. (2009). Influence of Patagonian glaciers on Antarctic dust deposition during the last glacial period. *Nature Geoscience*, *2*, 281–285.

Tegen, I., & Fung, I. (1994). Modeling of mineral dust in the atmosphere: Sources, transport, and optical thickness. *Journal of Geophysical Research*, *99*, 22,897–22,914. https://doi.org/10.1029/94JD01928

Veres, D., Bazin, L., Landais, A., Toyé Mahamadou Kele, H., Lemieux-Dudon, B., Parrenin, F., et al. (2013). The Antarctic ice core chornology (AICC2012): An optimized multi-parameter and multi-site dating approach for the last 120 thousands years. *Climate of the Past*, *9*, 1733–1748.

Wauben, W. M., Bitanja, R., van Velthoven, P. F., & Kelder, H. (1997). On the magnitude of transport out of the Antarctic polar vortex. *Journal of Geophysical Research*, *102*, 1229–1238. https://doi.org/10.1029/96JD02741

Weber, M. E., Kuhn, G., Sprenk, D., Rolf, C., Ohlwein, C., & Ricken, W. (2012). Dust transport from Patagonia to Antarctica—A new stratigraphic approach from the Scotia Sea and its implications for the last glacial cycle. *Quaternary Science Reviews*, *36*, 177–188.

Wegner, A., Fischer, H., Delmonte, B., Petit, J. R., Erhardt, T., Ruth, U., et al. (2015). The role of seasonality of mineral dust concentration and size on glacial/interglacial dust changes in the EPICA Dronning Maud Land ice core. *Journal of Geophysical Research: Atmospheres*, *120*, 9916–9931. https://doi.org/10.1002/2015JD023608

White, A. F., Bullen, T. D., Vivit, D. V., Schulz, M. S., & Clow, D. W. (1999). The role of disseminated calcite in the chemical weathering of granitoid rocks. *Geochimica et Cosmochimica Acta*, *63*, 1939–1953.

Yung, Y. L., Lee, T., Wang, C. H., & Shieh, Y. T. (1996). Dust: A diagnostic of the hydrologic cycle during the last glacial maximum. *Science*, *271*, 962–963.